Computational Modeling of Magnetic Intervention

D. V. Rose, T. C. Genoni, E. A. Madrid, R. E. Clark, D. R. Welch
Voss Scientific, LLC

A. E. Robson, J. D. Sethian, J. L. Giuliani and A. L. Velikovich
Naval Research Laboratory

High Average Power Laser Program Workshop
Madison, Wisconsin
October 22 and 23, 2008

Status report on computational modeling for Magnetic Intervention (MI):

- Refinements to the Bell Cusp (*A. Robson*) have been examined using ion orbit calculations:
  - *Several options for the ring cusp dump regions have been proposed (falls, pools)*
- A hydrodynamic analysis of the response of the liquid metal (*Pb*) pool and/or falls has been sketched out.
  - Several equation-of-state options have been examined (QEOS, Soft-Sphere, Van der Waals, etc.).
  - 1D hydrodynamic code development is underway.

Bell Cusp Concept (A. Robson):

- Bertie's design has two magnetic field modifications compared with the original MI cusp scheme:
  - Greatly increased coil currents at/near the point cusp to reduce the ion phase-space acceptance
  - An addition coil modifying the planar ring cusp to form a bell cusp

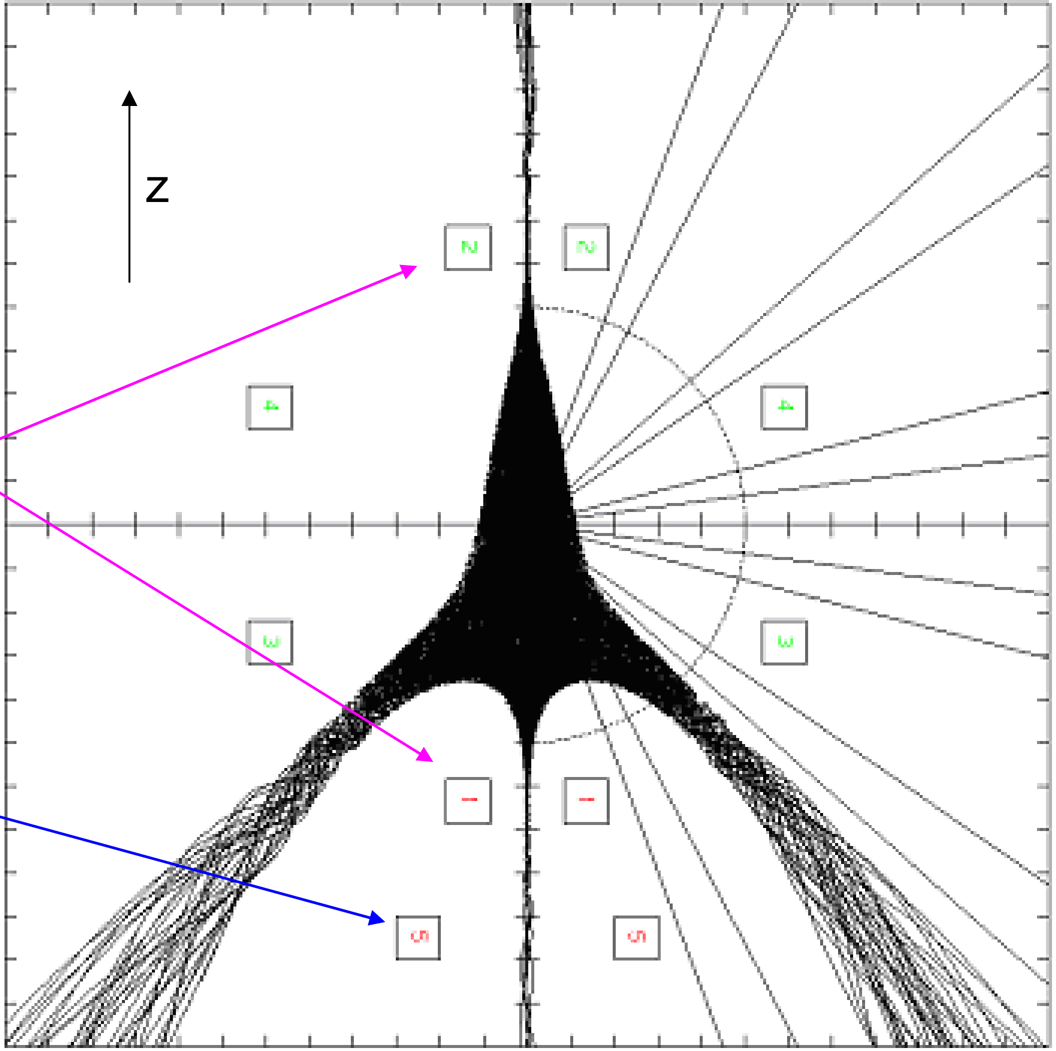

This scheme opens up a number of possible ion dump scenarios, including liquid pools, "water" (lead) falls, mists/vapors, etc.

Helium ion density at 20, 40, 60 μs times for the new 8-coil configuration:

- Ion channel width is relatively narrow far outside of the chamber.
- Additional transverse spreading likely is due to finite β effects inside of the chamber.
- Small-radius, well-focused ion streams are present along the point cusps.

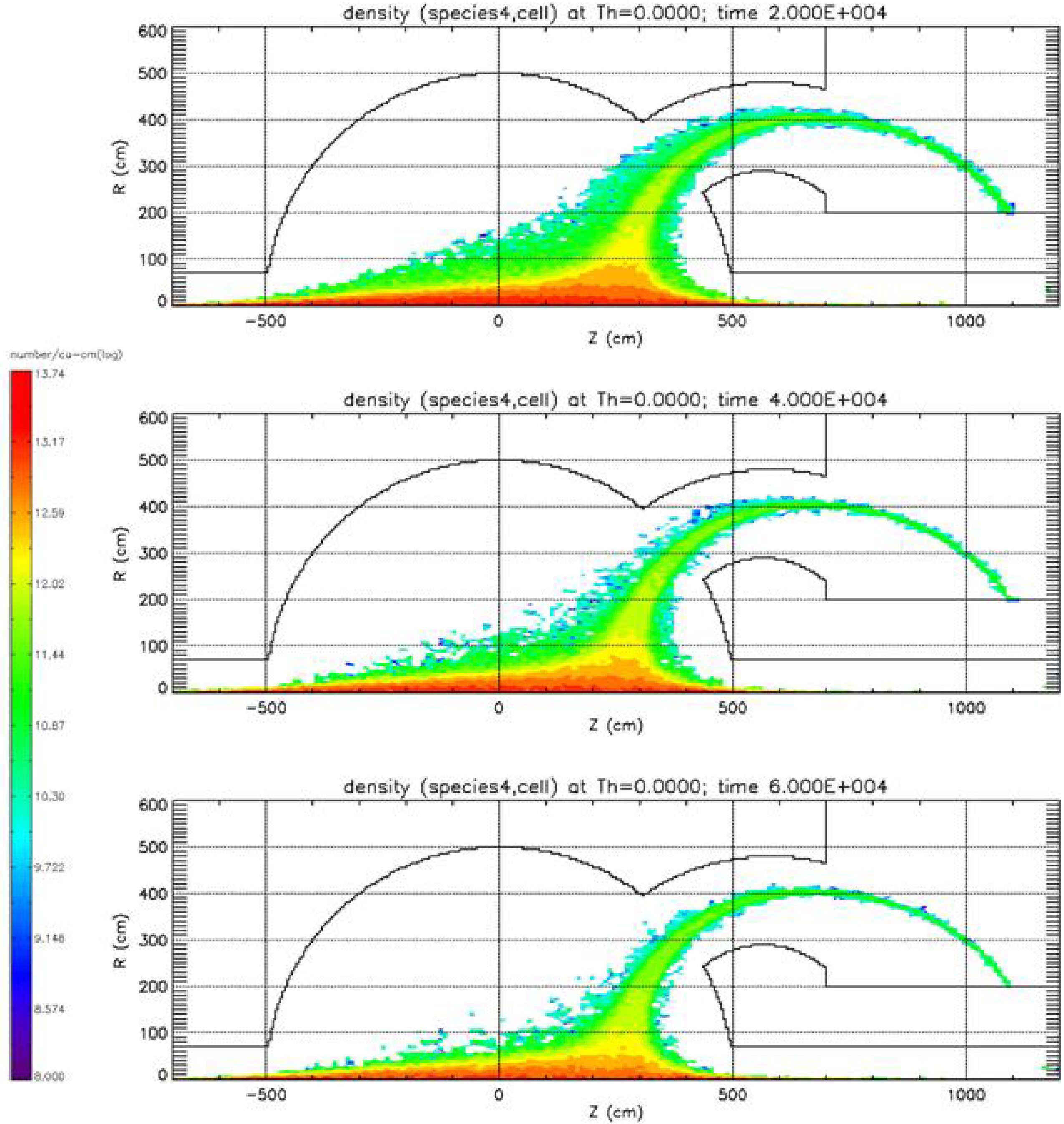

Bell Cusp Ion Deposition Profiles

- We use the orbit calculations to track in time and space the energy striking the dump region.
- The time-dependent energy deposited as a function of depth is then estimated using simple dE/dx ion stopping power functions.
- This gives a “depth-dose” profile that is the input to the hydrodynamic response model.

Escaping ion distribution at one plane in the Bell Cusp:

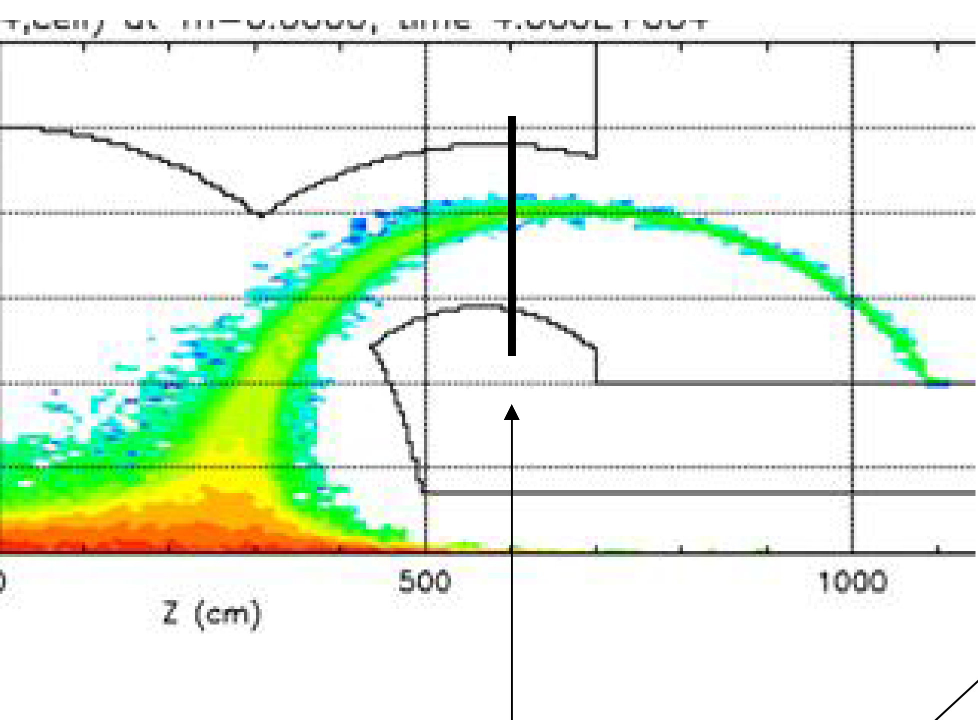

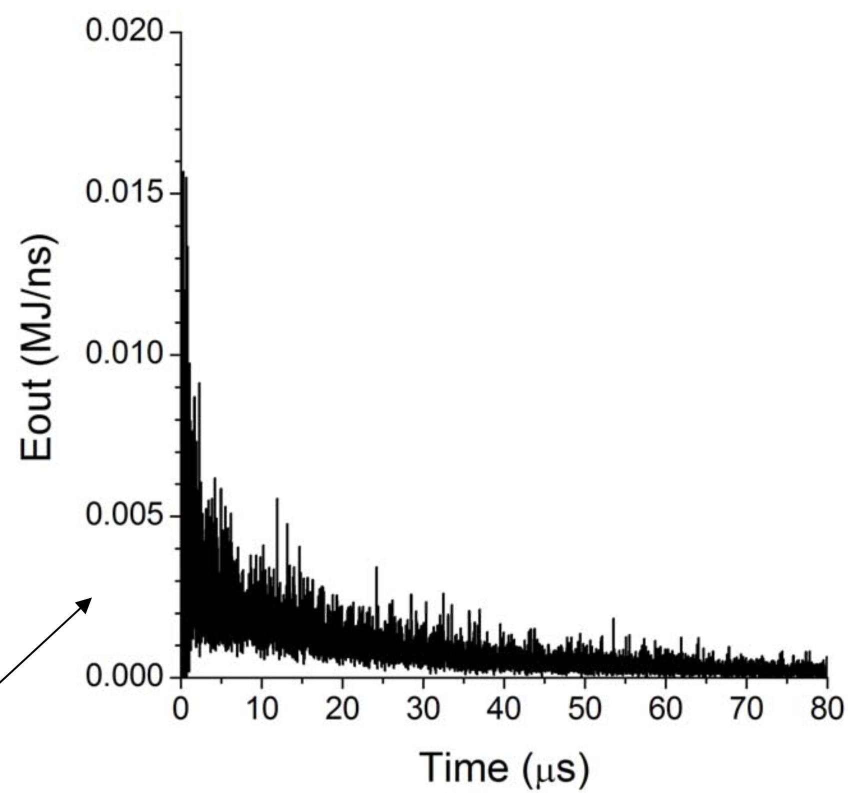

Diagnostic plane recording ion energy escaping the chamber as a function of time.

Sample Surface Deposition Profiles

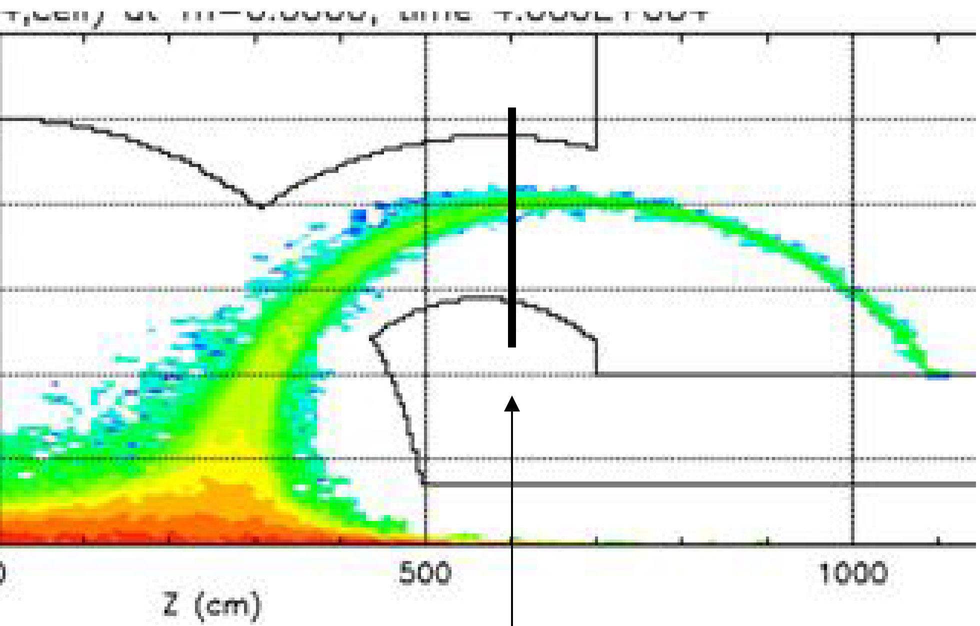

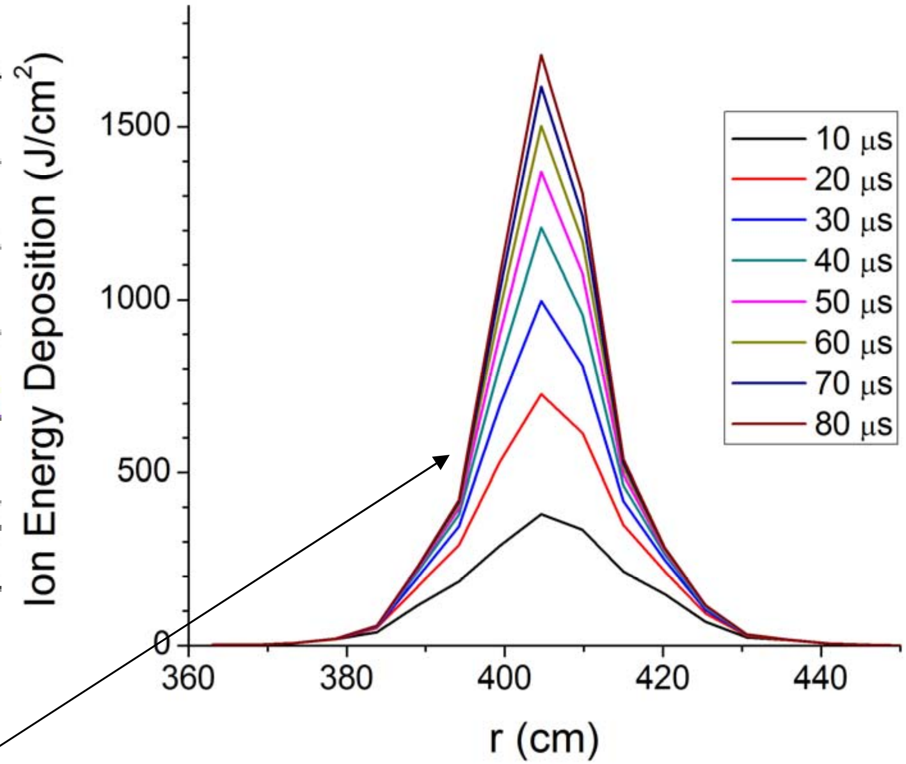

Diagnostic plane recording ion energy escaping the chamber as a function of time.

Time-integrated depth-dose profiles for escaping Bell-Cusp ions in Lead:

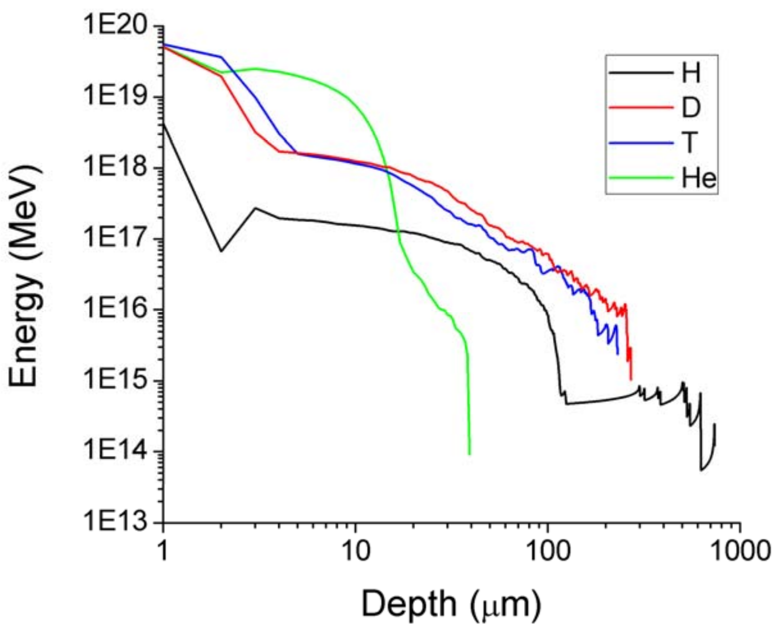

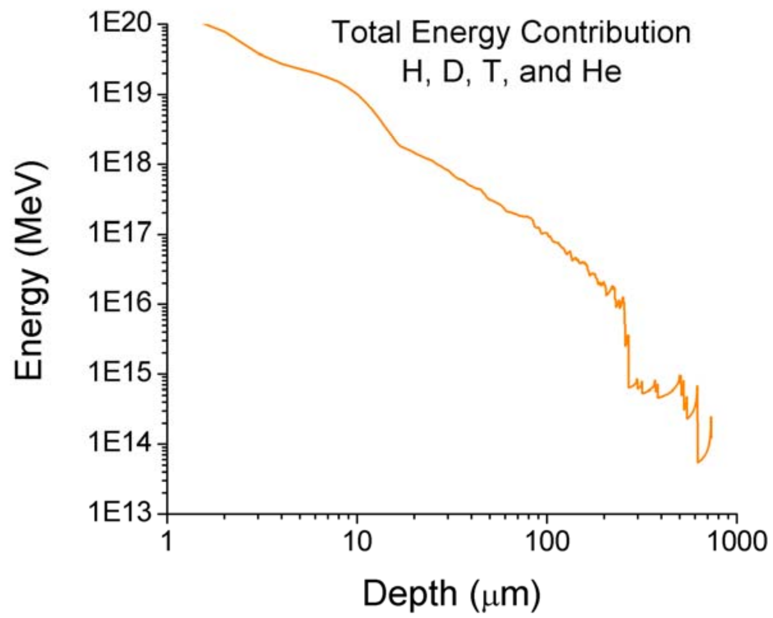

For crude energy density at the surface of the liquid, divide these values by your favorite cross-sectional area. (*e.g.* 12 m^2)

Depth-dose profiles in 10 μs groupings:

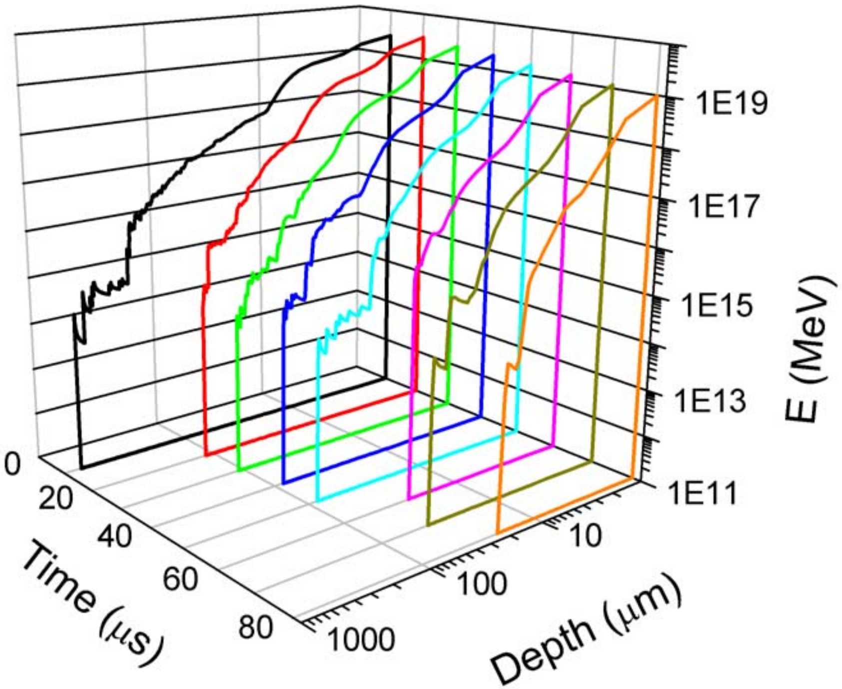

As expected, maximum deposition occurs in first ~10 microns.

Significant energy is deposited throughout the 80 μs times plotted.

3D views of the same data set on linear space and time scales illustrates the exponential time decay.

Linear Energy Scale

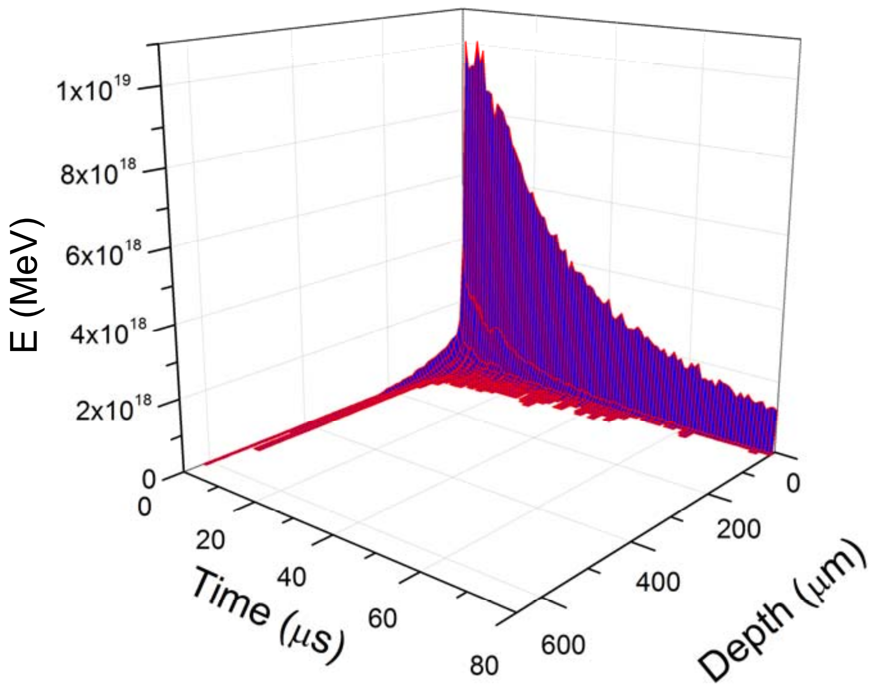

Log10 Energy Scale

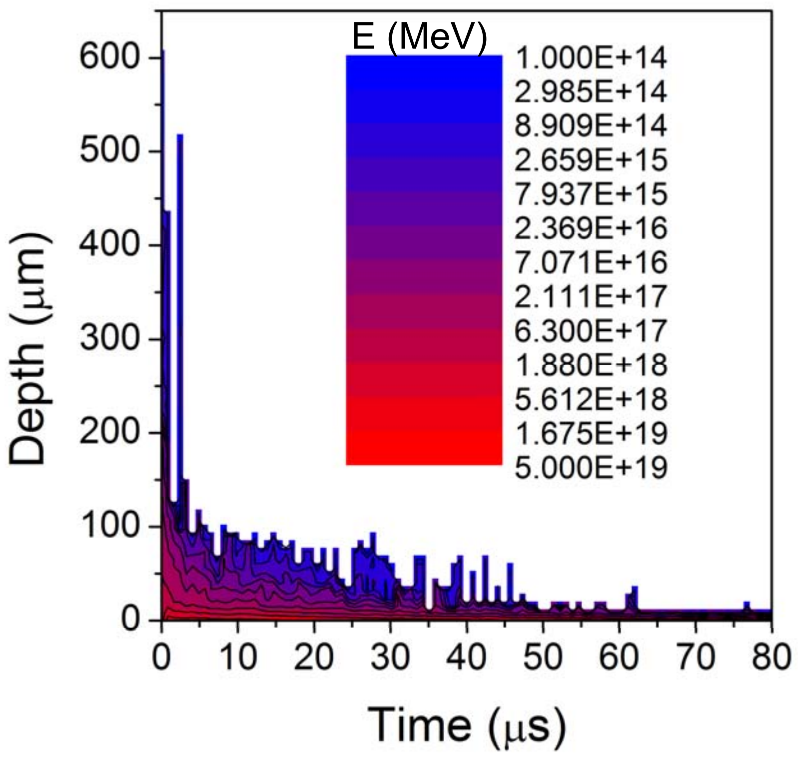

Material response calculations - ion beam deposition into liquid metal pool and/or falls.

- We seek a time-accurate numerical model of the response of a liquid metal layer to deposition of an intense ion flux (beyond the small-signal approximation).
- The model must address the phase transition at the vapor-liquid boundary as well as any shock propagation out of the opposite side of the liquid layer (substrate).
- Similar modeling has been carried out for short-duration (a few ns) energy pulses including MeV proton beams [Rogerson:1985] and *x*-rays [Zaghloul:2005].
- A. Velikovich has looked at the problem is a shock wave launched in 2-mm thick liquid lead propagating to a steel substrate [Velikovich:2008]. This analysis indicated that there the shock wave would not damage the steel.

1D Viscous Lagrangian Hydrodynamic Model:

Mass Continuity: $$\frac{d\rho}{dt} = -\rho \frac{\partial v}{\partial x},$$

Momentum: $$\rho \frac{dv}{dt} = -\frac{\partial P}{\partial x} + \frac{\partial}{\partial x}\left(\lambda \frac{\partial v}{\partial x} \right),$$

Energy: $$\frac{d\varepsilon}{dt} = \frac{P}{\rho^2}\frac{d\rho}{dt} + \frac{\lambda}{\rho}\left(\frac{dv}{dx} \right)^2 + \frac{1}{\rho}\frac{\partial}{\partial x}\left(\kappa \frac{\partial T}{\partial x} \right),$$

Displacement: $$\frac{dx}{dt} = v,$$

Here λ is the *bulk viscosity*, and κ is the *thermal conductivity*.
We assume these are scalars in the following finite difference formulas.

Momentum Equation Finite Difference Form:

$$\frac{v_k^{n+1/2} - v_k^{n-1/2}}{\Delta t^n} = -\frac{P_{k+1/2}^n - P_{k-1/2}^n}{\Delta m_k} + \frac{\lambda}{\Delta m_k}\left[\frac{v_{k+1}^n - v_k^n}{\Delta m_{k+1/2}}\rho_{k+1/2}^n - \frac{v_k^n - v_{k-1}^n}{\Delta m_{k-1/2}}\rho_{k-1/2}^n\right]$$

$$dm = \rho dx$$

$$\Delta m_k \equiv \frac{1}{2}\left(\Delta m_{k+1/2} + \Delta m_{k-1/2}\right)$$

$$v_k \equiv \frac{1}{2}\left(v_k^{n+1/2} + v_k^{n-1/2}\right)$$

Definitions – see next slide.

Unknowns are $v^{n+1/2}$ terms which form a coupled tri-diagonal system.

Computational Grid:

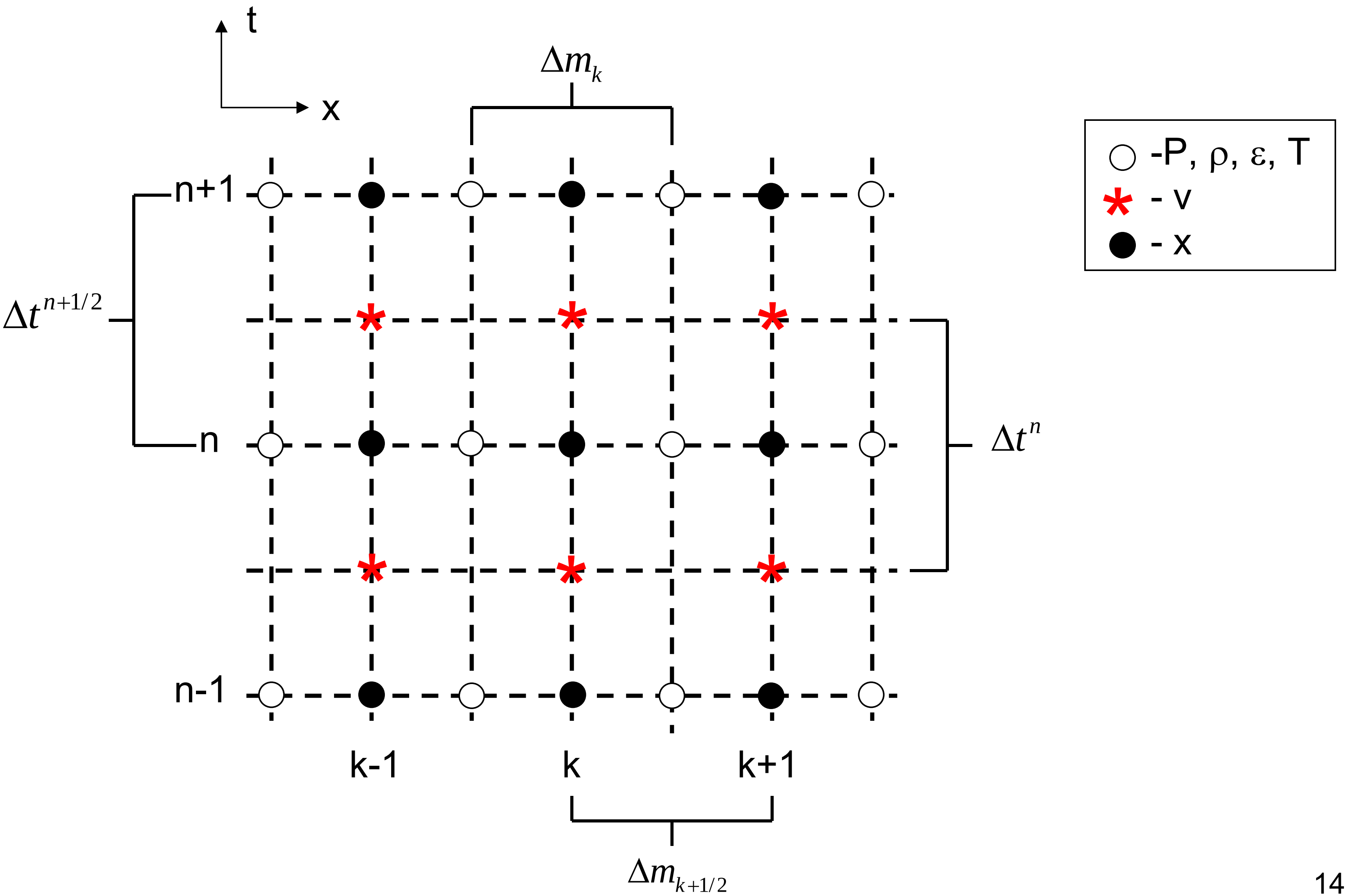

Finite difference forms for the displacement, mass continuity, and energy equations:

$$x_k^{n+1} = x_k^n + v_k^{n+1/2} \Delta t^{n+1/2}$$ Displacement

$$\frac{1}{\rho_{k+1/2}^{n+1}} = \frac{x_{k+1}^{n+1} - x_k^{n+1}}{\Delta m_{k+1/2}}$$ Mass Continuity

For the energy equation, we assume EOS data in the form:

$$\varepsilon = \varepsilon(\rho, T)$$

$$P = P(\rho, T)$$

as well as the derivatives

$$\partial\varepsilon / \partial\rho$$

$$\partial\varepsilon / \partial T$$

The energy equation can be expressed in the following "temperature" form:

$$\frac{\partial\varepsilon}{\partial T}\frac{dT}{dt} = \frac{\partial\varepsilon}{\partial\rho}\rho^2 \frac{\partial v}{\partial m} - P\frac{\partial v}{\partial m} + \lambda\rho\left(\frac{\partial v}{\partial m}\right)^2 + \kappa\frac{\partial}{\partial m}\left(\rho\frac{\partial T}{\partial m}\right)$$

Finite difference form of the energy equation:

$$\left(\frac{\partial\varepsilon}{\partial T}\right)_{k+1/2}^{n+1/2}\frac{T_{k+1/2}^{n+1}-T_{k+1/2}^{n}}{\Delta t^{n+1/2}}=\left(\frac{\partial\varepsilon}{\partial\rho}\right)_{k+1/2}^{n+1/2}\left(\rho_{k+1/2}^{n+1/2}\right)^2\left[\frac{v_{k+1}^{n+1/2}-v_{k}^{n+1/2}}{\Delta m_{k+1/2}}\right]$$

$$-P_{k+1/2}^{n+1/2}\left[\frac{v_{k+1}^{n+1/2}-v_{k}^{n+1/2}}{\Delta m_{k+1/2}}\right]+\lambda\rho_{k+1/2}^{n+1/2}\left[\frac{v_{k+1}^{n+1/2}-v_{k}^{n+1/2}}{\Delta m_{k+1/2}}\right]^2$$

$$+\frac{\kappa}{\Delta m_{k+1/2}}\left[\frac{T_{k+3/2}^{n+1/2}-T_{k+1/2}^{n+1/2}}{\Delta m_{k+1}}\rho_{k+1}^{n+1/2}-\frac{T_{k+1/2}^{n+1/2}-T_{k-1/2}^{n+1/2}}{\Delta m_{k}}\rho_{k}^{n+1/2}\right]$$

The above uses the following definitions:

$$\rho_{k+1/2}^{n+1/2}\equiv\frac{1}{2}\left[\rho_{k+1/2}^{n+1}+\rho_{k+1/2}^{n}\right],$$

$$\rho_{k}^{n+1/2}\equiv\frac{1}{4}\left[\rho_{k+1/2}^{n+1}+\rho_{k+1/2}^{n}+\rho_{k-1/2}^{n+1}+\rho_{k-1/2}^{n}\right],$$

$$T_{k+1/2}^{n+1/2}\equiv\frac{1}{2}\left[T_{k+1/2}^{n+1}+T_{k+1/2}^{n}\right],$$

$$\left(\frac{\partial\varepsilon}{\partial T}\right)_{k+1/2}^{n+1/2}=\frac{1}{2}\left[\frac{\partial\varepsilon\left(\rho_{k+1/2}^{n+1},T_{k+1/2}^{n+1}\right)}{\partial T}+\frac{\partial\varepsilon\left(\rho_{k+1/2}^{n},T_{k+1/2}^{n}\right)}{\partial T}\right],$$

$$\left(\frac{\partial\varepsilon}{\partial\rho}\right)_{k+1/2}^{n+1/2}=\frac{1}{2}\left[\frac{\partial\varepsilon\left(\rho_{k+1/2}^{n+1},T_{k+1/2}^{n+1}\right)}{\partial\rho}+\frac{\partial\varepsilon\left(\rho_{k+1/2}^{n},T_{k+1/2}^{n}\right)}{\partial\rho}\right],$$

$$P_{k+1/2}^{n+1/2}=\frac{1}{2}\left[P\left(\rho_{k+1/2}^{n+1},T_{k+1/2}^{n+1}\right)+P\left(\rho_{k+1/2}^{n},T_{k+1/2}^{n}\right)\right]$$

Energy equation solution:

We anticipate solving the energy equation by first "guessing" the values of T^{n+1} (simply use the previous time step values) and then evaluate

$\partial\varepsilon / \partial T$, $\partial\varepsilon / \partial\rho$, and P at (k+1/2,n+1/2).

The tri-diagonal system is solved for T^{n+1}, and then iterated until suitable convergence is achieved.

EOS Models:

- There are several choices available to us for EOS models of liquid metals:

  – QEOS [More:1988]: We are developing our own numerical implementation of this model which handles liquid→vapor phase transition and hot vapor equilibrium charge-states using the Thomas-Fermi model.

  – Soft-Sphere Model [Young:1977]: Liquid→vapor transitions.
  Used by Zaghloul and Raffray [Zaghloul:2005] for examining response of thin liquid (Pb) layer to prompt x-ray burst in an IFE chamber.

  – DGSS [Giuliani:2008]: Debye-Gruneisen solid-state model combined with the Soft-Sphere model developed by John Giuliani.

- There are significant discrepancies among the various model results. These include the liquid-vapor phase boundary/saturation pressure as a function of temperature, the critical temperature, pressure, and volume. These differences should be sorted out to give a consistent picture.

Sample EOS model data [Giuliani:2008]

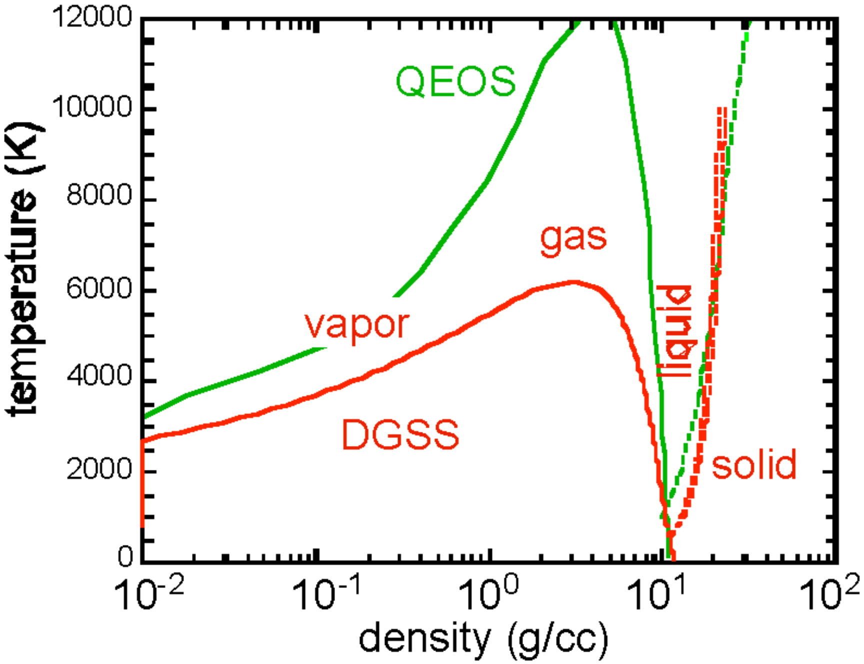

Solid-liquid and liquid-vapor co-existence curves for lead in the (ρ,T) plane from the DGSS model along with the corresponding phase states (red). Liquid-vapor co-existence curves from the QEOS model (green).

(Note the large QEOS/DGSS discrepancy in the co-existence curves.)

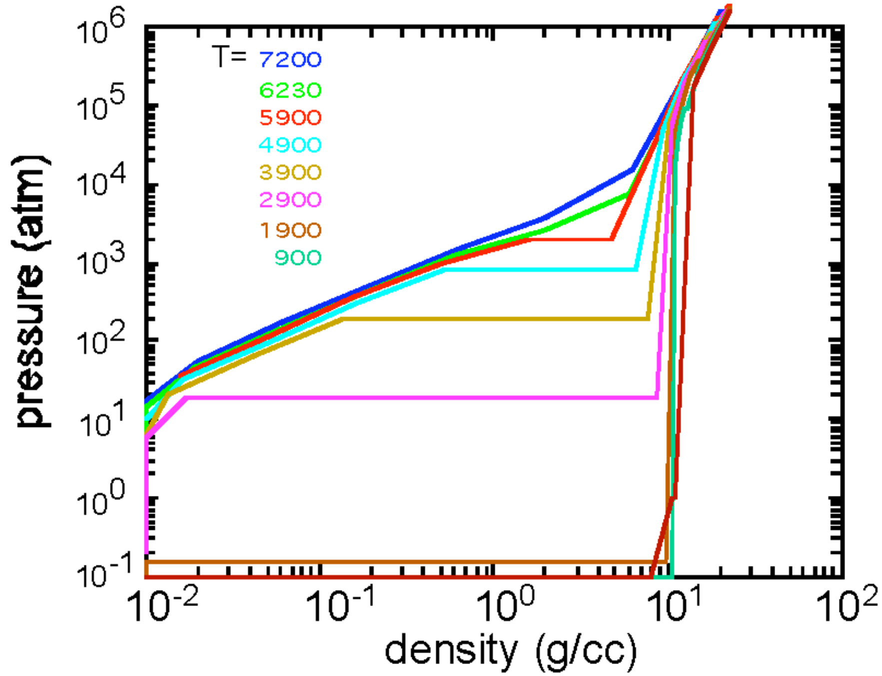

Pressure along denoted isotherms from the DGSS model.

Horizontal lines indicate liquid-vapor phase co-existence region (from Maxwell construction).

Caveats, issues

- Radiation transport – must be considered as well as part of the overall analysis.

- Response of the substrate for the case of a thin-liquid layer – can a shock induced by the ion deposition fatigue/damage the substrate? (*The Velikovich analysis indicates that it will not be an issue*.)

- All hydrodynamic calculations should be carried out for a range of input energy-densities to account for uncertainties in expected ion escape energies and channel widths.

Summary:

- We are beginning a study of the hydrodynamic response of a liquid metal layer to an intense ion energy pulse.
- We have mapped out a finite-difference scheme for solution of the 1D viscous Lagrangian hydrodynamic equations including boundary conditions to model both the liquid-vapor transition and the liquid-wall interface.
- We are examining several EOS models applicable to liquid metals (e.g. lead).
- The ion energy pulse has been characterized as a depth-dose profile using orbit calculations of the Bell Cusp geometry.

References:

- [Giuliani:2008] J. L. Giuliani, “Lead equation-of-state for the chamber dumps,” unpublished memorandum, October 3, 2008.
- [More:1988] R. M. More, K. H Warren, D. A. Young, and G. B. Zimmerman, “A new quotidian equation of state (QEOS) for hot dense matter,” Phys. Fluids **31**, 3059 (1988).
- [Rogerson:1985] J. E. Rogerson, R. W. Clark, and J. Davis, “Ion-beam deposition, heating, and radiation from an aluminum plasma,” Phys. Rev. A **31**, 3323 (1985).
- [Velikovich:2008] A. L. Velikovich, “Effect of ion deceleration in liquid lead on a steel substrate,” unpublished memorandum, 2008.
- [Young:1977] D. A. Young, “A soft sphere model for liquid metals,” LLNL Report UCRL-2352 (1977).
- [Zaghloul:2005] M. R. Zaghloul and A. R. Raffray, “IFE liquid wall response to the prompt x-ray energy deposition: investigation of physical processes and assessment of ablated material,” Fusion Sci. Technol. **47**, 27 (2005).